Seismic Structure Studies of the Pine River Gas Seep Area, La Plata County, Colorado

By A. Curtis Huffman, Jr. and David J. Taylor

INTRODUCTION

The objective of this part of the study was to determine what influence deep-seated controls might have exerted on fracturing and faulting in the Fruitland Formation and related rocks in La Plata County. In order to hold down costs, the investigation was limited to existing seismic and drill hole data in the vicinity of the Los Pinos River. The USGS had a seismic reflection line owned by Maxus Exploration Company (Natomas line AAC-1, 2,and 3) from a previous study and Amoco Production Company contributed three shallow high-resolution seismic reflection lines (HXS-1,-2,-3). The recording parameters of the Maxus line were designed to best resolve reflectors at depth (Pennsylvanian) while the Amoco lines were designed to resolve the shallow (Cretaceous) reflectors best. Fortunately, one of the Amoco lines (HXS-3) was recorded coincident with part of Maxus line 1 which enabled us to superimpose the two, thus recovering detail from the entire section, not possible using either of the lines separately. However, due to the lack of detail and accuracy on the shot-point map we received from Amoco, we are unable to precisely correlate the two lines nor are we able to accurately describe or locate any interpreted features. Also, because we had no east-west seismic lines in the area, we are unable to fully describe the geometry of the interpreted features.

In addition to the seismic lines, Amoco also made available an unpublished 1994 report, “Pine River Fruitland Coal Outcrop Investigation”, put together by the Southern Rockies Business Unit of Amoco Production Company. K.N. Energy Inc. contributed three seismic lines acquired by Fuelco. These lines were too far away from the area of study to be directly applicable but were of considerable use in obtaining a regional perspective because they were also designed to resolve the shallow part of the section and were far enough removed from the basin margin faulting that we could use them for comparative purposes. Also useful were previous studies performed by the authors in various parts of the San Juan Basin.

Thrust faulting underlying the Hogback Monocline along the northwestern rim of the San Juan Basin was first described by Taylor and Huffman (1988) and this interpretation was later expanded to include the monoclines along the northern and northeastern rims (Huffman and Taylor, 1989). Huffman and Taylor (1989) also reported an orthogonal pattern of basement faulting throughout the San Juan Basin. This pattern is reflected in the overlying sedimentary section and has influenced the occurrence and production of energy resources throughout the basin (Huffman and Taylor, 1991). Huffman and Condon (1993) used these faults to help explain Pennsylvanian and Permian depositional patterns. Analysis of effects on Cretaceous deposition and structure, however, has been largely conjecture primarily due to the lack of good seismic data in the shallower part of the section. The lines supplied by Amoco are the first high resolution seismic data we have been able to work with and although the data have serious shortcomings, they have provided new insights into the structure and tectonic style along the margins of the basin.

SEISMIC AND BOREHOLE DATA

As part of the La Plata County study, the U.S. Geological Survey received three shallow high resolution seismic lines from Amoco. A coarse location map, paper copies of the lines, and digital SEG-Y tapes of the processed data were also included. The USGS asked for, and did receive, copies of the side labels for the seismic lines.

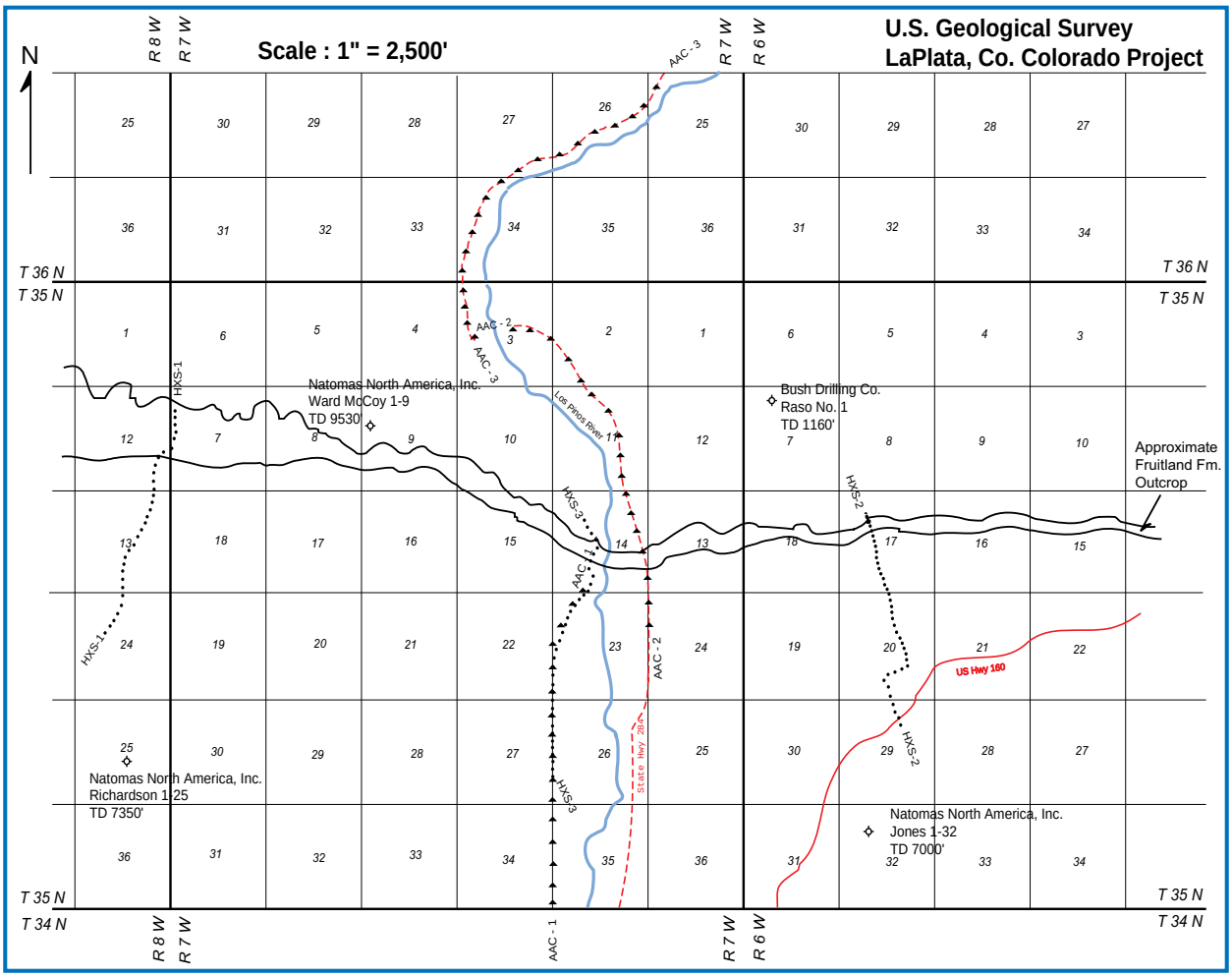

Figure 3-1. Map showing location of well and seismic data used in the study.

This provided us with acquisition information needed in order to perform additional processing on the seismic data.

Using the Landmark/Advance ProMAX seismic data processing system we re-displayed all three lines at a common scale. Unfortunately, we could not correlate the CDP numbers from the SEG-Y headers on tape with the shot numbers on both the location map and the original paper copies of the data. Therefore, we were forced to estimate the correlation between the shot locations from the map and the seismic data. The resulting configuration is shown in figure 3-1 and, although we recognize that the positions are not exact, we feel confident that they allow a reasonably accurate representation of the data.

Synthetic seismograms generated from logs for the following four wells were used to correlate subsurface horizons with seismic reflectors. Locations of the wells are shown in figure 3-1.

Natomas North America Inc.
Ward McCoy 1-9
SW of the NW: T35N, R7W, Section 9
TD 9,350'

Natomas North America Inc.
Richardson 1-25
NW of the SE: T35N, R8W, Section 25
TD 7,350'

Natomas North America Inc.
Jones 1-32
SE of the NW: T35N, R6W, Section 32
TD 7,000'

Bush Drilling Company
Raso 1
NE of the NW: T35N, R6W, Section 7
TD 1,160'

The McCoy well is located about 2 miles east of the north end of seismic line HXS-1 and 2.3 miles west-northwest of the north end of seismic line HXS-3. The Richardson well is located approximately 1.2 miles south of the southern end of seismic line HXS-1 and 4.5 miles west of the southern end of seismic line HXS-3. The Jones well is located about 1 mile south of the southern end of seismic line HXS-2 and 3.3 miles east-southeast of the southern end of seismic line HXS-3. The Raso well is located 1.5 miles northwest of the northern end of seismic line HXS-2.

SYNTHETIC SEISMOGRAMS

A synthetic seismogram is generated by calculating a reflection coefficient series from an acoustic velocity log (and optionally, a density log) measured in a borehole. The reflection coefficient series is then convolved with an estimate of the seismic source waveform to produce the final synthetic seismic response. The object is to create a close match between the synthetic seismogram and the surface seismic section. Once the match is made identification of reflecting interfaces observed on the surface seismic section can be made.

A reflection coefficient is defined as the ratio of the amplitude of a reflected wave to that of the incident wave. For normal incidence on an interface which separates media of densities (gm/cc) p_n and p_{n+1} and velocities (ft./sec.) V_n and V_{n+1}, the reflection coefficient can be calculated by:

$$(p_{n+1} V_{n+1} - p_n V_n) / (p_{n+1} V_{n+1} + p_n V_n)$$

where n is the sample number of the density or acoustic velocity log.

In the absence of a measured density log, we can use a constant value for the density, or density can be estimated using a number of empirical relationships between velocity and density. Similarly in the absence of a measured acoustic velocity log a sonic log can be estimated using one of several empirical relationships between resistivity measurements and acoustic velocity.

Sonic and density logs were digitized for the Jones well. A sonic log was digitized for the Raso well, but no density log was available. No sonic logs were available for the McCoy and Richardson wells, so the dual induction - SFL logs were digitized for these wells instead. Sonic logs were generated from these resistivity logs using Faust's equation (Faust, 1951 and Faust, 1953) as described below.

$$10^6 / \text{SONIC} = 1948 (Z^{1/6}) (R^{1/6})$$

or

$$\text{SONIC} = 1948 (Z^{1/6}) (R^{1/6}) / 10^6$$

where "Z" is the depth in feet "R" is the resistivity value in ohms at that depth, and "SONIC" is the resultant acoustic velocity value in μs/ft.

The Raso well did not have a density log available so a conversion was used to create one from the sonic log. Using Lindseth's equation (Lindseth, 1979), described below, a pseudo density log in gm/cc was generated.

$$p = (V-3460) / (V(.308))$$

where *"p"* is the density value in gm/cc and "V" is the compressional wave velocity in ft/sec which is derived using the equation:

$$V \text{ (ft/sec)} = 10^6/\text{SONIC } (\mu s/ft)$$

Sonic and density values were used to produce the impedance and reflection coefficient logs. Figures 3-2 through 3-5 are plots of the various logs used to create the reflectivity series with geologic tops annotated. Sonic logs were also used to create depth, and velocity logs.

Figure 3-6 is a plot of the wavelet used to generate the synthetic seismograms. It is a zero phase bandpass wavelet with a frequency content of 12 to 55 hertz. This wavelet matches the primary frequency content of the seismic data. Because the seismic data has been deconvolved, a zero phase wavelet is appropriate. Figure 3-7 is a plot showing all of the final synthetic seismograms for the four wells used in the study.

SEISMIC DATA—PROCESSING

As mentioned previously, the U.S. Geological Survey received three shallow high-resolution multichannel seismic lines from Amoco. Initial examination of the data showed that these lines were processed through CDP stack with no

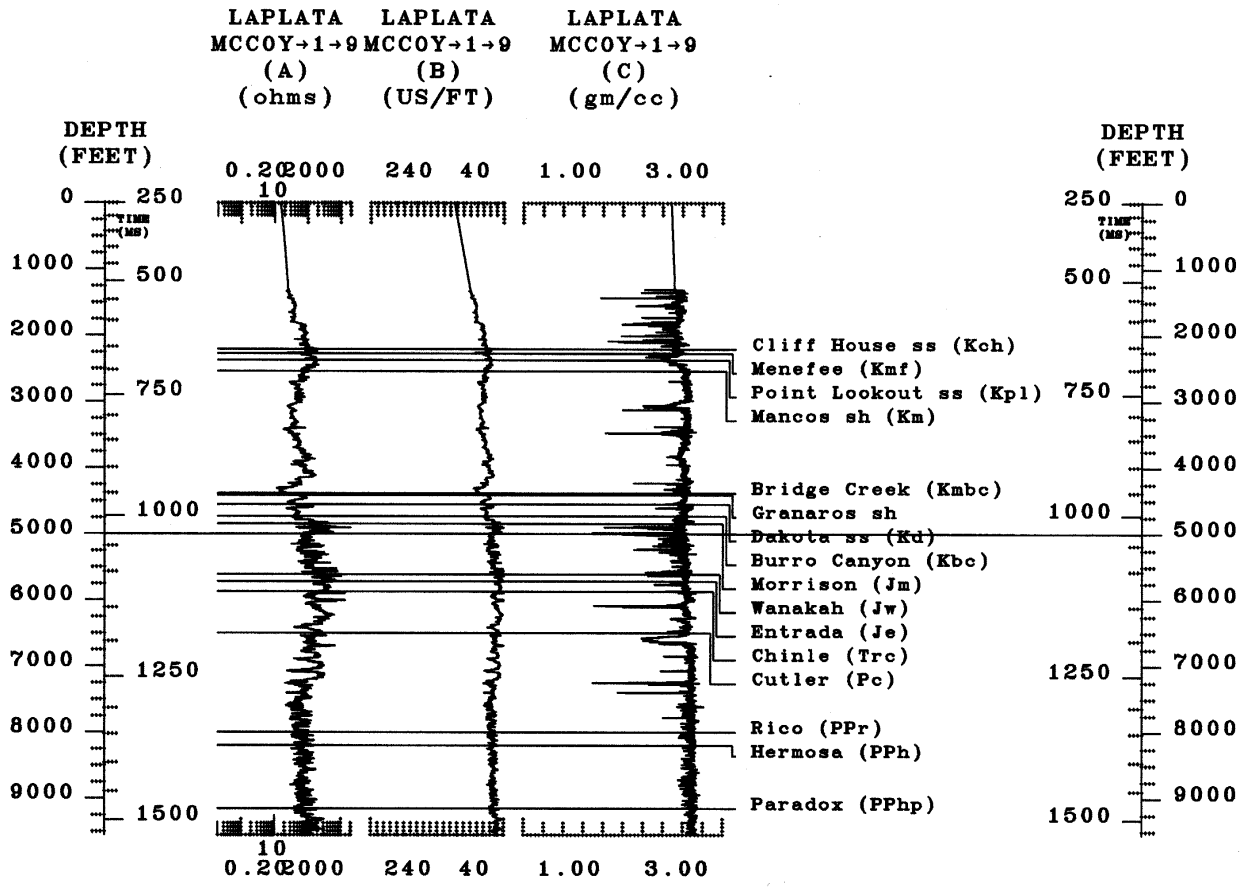

Figure 3-2. Display of the (A) measured resistivity log, (B) sonic log generated using Faust's equation, and (C) density log generated from the sonic log utilizing Lindseth's equation used to generate a synthetic seismogram for the Ward McCoy No. 1-9 well.

migration applied. There was also a significant amount of noise in the section and what we interpreted to be interbed multiples below the strong reflectors of the Dakota Formation.

We used several post-stack processing techniques in an effort to decrease the noise content of the data without degrading the signal. These included spike and noise burst reduction, F-X deconvolution, and bandpass filtering. All of these processes attacked a specific noise problem and produced a section that was easier to interpret after they were applied. The post-stack processing sequence included:

*SEG-Y Tape Input
*Disk Data Input
*Spike Burst Edit
*Noise Burst Edit
*F-X Deconvolution
*Bandpass Filter (8-12-55-60 Hz.)
*Automatic Gain Control
*Disk Data Output

Once a satisfactory stacked section was produced, the data were migrated to collapse the diffractions and move the reflectors to their true subsurface location using a Kirchoff time migration algorithm.

Because the original field data were not available to us we could not determine migration velocities directly from the seismic data, therefore, we converted the sonic and velocity information from the wells to RMS velocities and used the results for the migration. Key reflecting horizons were picked and the RMS velocities within those horizons were averaged. The averaged RMS velocities were then held constant across the section but the application time window was varied according to the dip of the key reflecting horizons. This procedure produced a satisfactory result as the section did not seem to be severely under or over migrated. The horizons and the averaged RMS velocities used were:

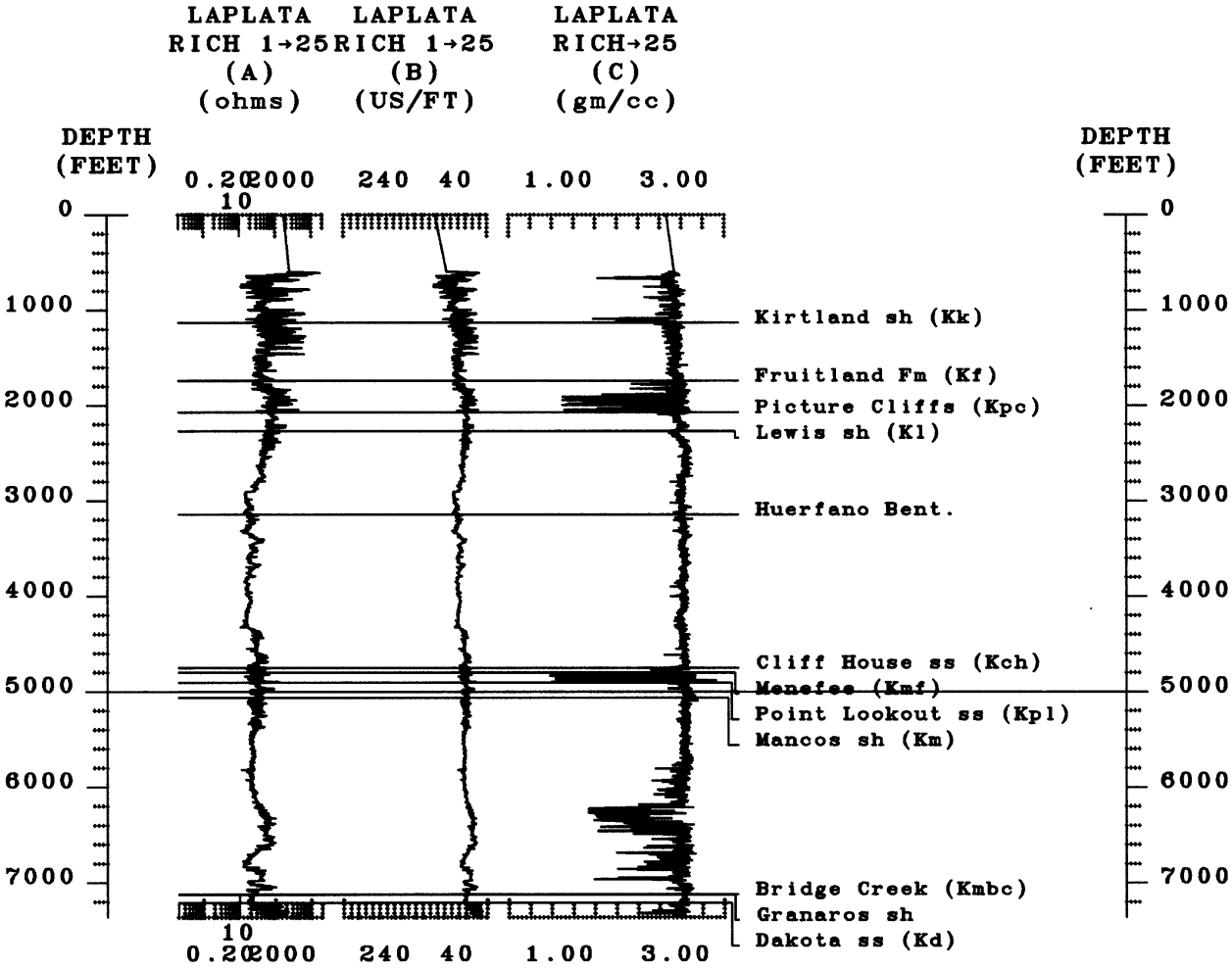

Figure 3-3. Display of the (A) measured resistivity log, (B) sonic log generated using Faust's equation, and (C) density log generated from the sonic log utilizing Lindseth's equation used to generate a synthetic seismogram for the Ward McCoy No. 1-9 well.

Top of Data	8860 ft/sec. (2700 m/sec.)
Top of Lewis Shale	10700 ft/sec. (3261 m/sec.)
Base of Lewis Shale	11400 ft/sec. (3475 m/sec.)
Dakota Formation	13000 ft/sec. (3962 m/sec.)
Cutler Formation	14650 ft/sec. (4465 m/sec.)
Paradox Formation	15420 ft/sec. (4700 m/sec.)
Base of Data	18500 ft/sec. (5639 m/sec.)

The following post migration processing was performed.

*Disk Data Input
*Trace Muting (mute pattern duplicated from Amoco processed sections)
*Bandpass Filter (8-12-60-64 Hz.)
*Automatic Gain Control

Final results were displayed at various scales. A scale of 10 inches per second two-way travel time in the vertical direction and 20 traces per inch in the horizontal direction proved to be the best for the interpretation.

SEISMIC DATA—INTERPRETATION

Line figure interpretations of the Amoco lines are shown in figures 3-8, 3-9, and 3-10. Several features are common to all of the Amoco lines: (1) the Dakota sandstone is a strong continuous reflector with few discontinuities; (2) the Fruitland Formation is a strong continuous reflector with few discontinuities; (3) there is little thickness change between the Dakota and the Fruitland except at the northern end of each line; (4) the Mancos and Lewis shales are highly deformed in the northern and central portions of each line and; (5) the Mesaverde Group is broken

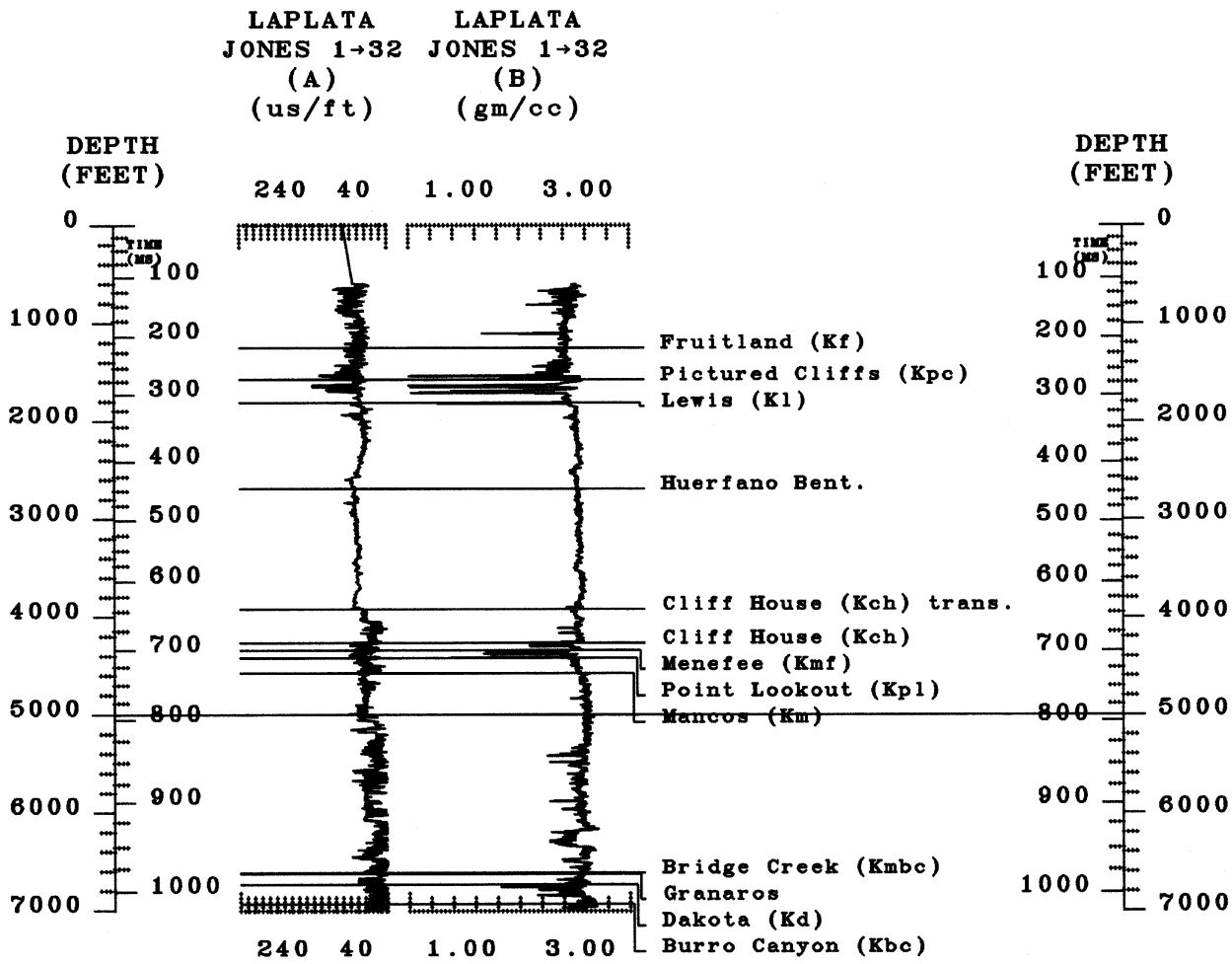

Figure 3-4. Display of the (A) measured sonic log and (C) density log generated from the sonic log utilizing Lindseth's equation used to generate a synthetic seismogram for the Jones No. 1-32 well.

and offset in a number of places on all lines. We interpret these features to indicate a certain amount of into-the-basin movement along glide planes in the shales with associated thrust faulting and back thrusting related to thrust faulting underlying the basin margin monocline.

Some of the apparently uplifted or downdropped (but not actually faulted) portions of certain reflectors, such as that in the Fruitland in the central part of line HXS-3, (fig. 3-10) could be attributed to: (1) a parallel fault underlying the line such that the line passes back and forth across the fault or; (2) to two separate faults at depth crossing the line at some angle. Such ambiguities cannot be totally resolved without a line at right angles to HXS-3. In this particular case, we prefer the underlying parallel fault interpretation because the apparent lithologic character of the Fruitland is the same on either side of the uplifted block but different from that within the block which would be more likely if the two downfaulted sides were actually part of a continuous section rather than two separate fault blocks. The Maxus line was of no help in this case because of data degradation at the ends of two of the line segments (AAC 1 and 2) immediately beneath the structure. In what may be a similar situation, the Dakota is offset by either a single underlying parallel fault or two cross-cutting faults in the southern part of line HXS-2 (fig. 3-9).

The northernmost end of line HXS-3 intercepts the basin margin thrust fault as well as a rather complicated set of thrusts and back thrusts associated with it. These associated faults also suggest that the apparent north verging reverse fault noted by Condon in this report could be a

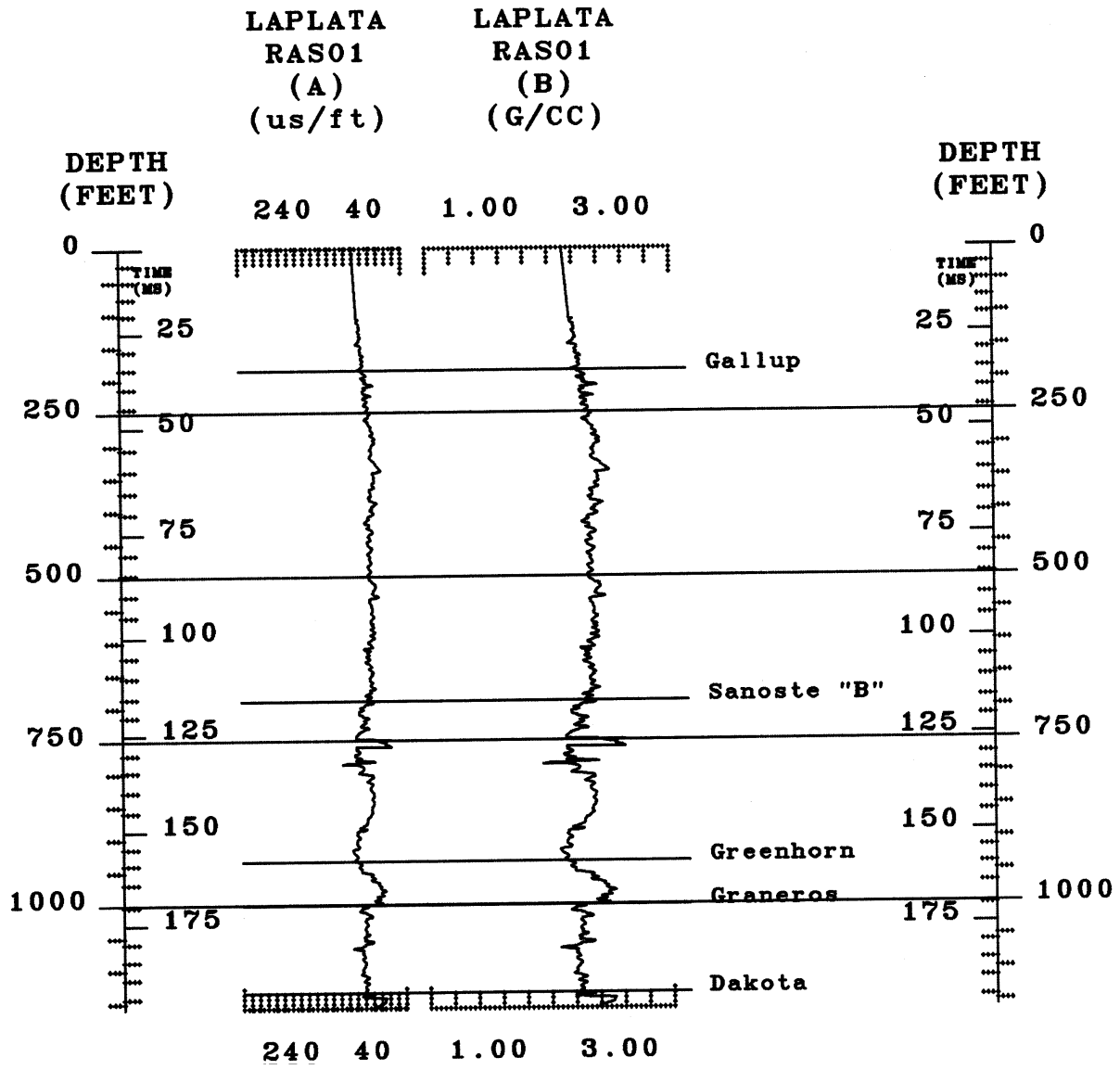

Figure 3-5. Display of the (A) measured sonic log and (C) density log generated from the sonic log utilizing Lindseth's equation used to generate a synthetic seismogram for the Raso No. 1 well.

back thrust (it should be noted that these interpretations are first approximations and only serve to illustrate the style and complexity of the structure).

Many lithologic variations can be seen, particularly in the Fruitland and Mesaverde of line HXS-3, as well as in the Mancos and Lewis shales of all the lines. Tongues of sand and shale enter the northern end of the marine units in all of the lines, particularly in the Lewis Shale, and we have interpreted a number of channels or delta lobes in the continental and marginal marine parts of the section. Some of the lithologic changes may have been localized by faulting at depth but most are probably the result of the position of the area within the Cretaceous seaway.

We interpret the apparent thickening between the Dakota and the Fruitland seen in the northern portion of the lines, particularly line HXS-2 (fig. 3-9), to be primarily tectonic in origin. South verging thrust faults related to the basin margin thrust are most prominent in HXS-2 but are present in the other lines as well. The overall effect of thrust faulting is to thicken the section; the basin margin thrusts interpreted in HXS-2 have caused a dramatic thickening in the Upper Cretaceous part of the section.

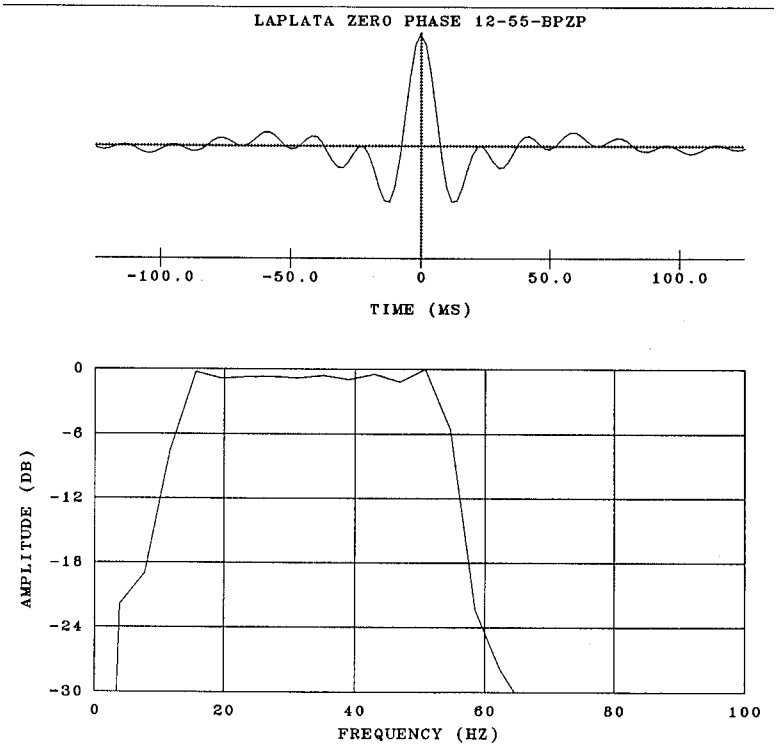

Figure 3-6. Plot showing the shape and frequency spectrum of the wavelet utilized to generate the synthetic seismograms for all of the wells used in the study area.

Line HXS-1 (fig. 3-8) contains the best evidence for a glide plane in the basal Mancos Shale. Thrust faults coming off this detachment surface, as well as associated back thrusts, break the Mesaverde into a number of blocks and significantly disrupt the Lewis Shale.

The only large though-going faults seen on any of the seismic lines available to this study are associated with the basin margin thrusting that underlies the monoclinal folding on three sides of the San Juan Basin. These thrust faults are typically multiple faults as they approach the surface (Taylor and Huffman,1988) and one or more of the branches may be seen to offset the Fruitland near the outcrop (figs. 3-8 and 3-9). We would expect a greater degree of fracturing in the vicinity of these faults than might otherwise be present. We can not comment on the probability of any north-south striking faults because of the absence of any east-west oriented data. The vicinity of the wind and water gaps and areas of changes in direction of the hogback would be likely places to look for such faults.

CONCLUSIONS

Little information specific to fracturing was gathered during the course of this study. The original intent was to compare faulting at depth to fracturing at the Fruitland Formation level and above. For the reasons cited previously, we were unable to map the faulting in the area so we were unable to compare the fracture patterns determined in other parts of this study with underlying fault patterns. Based on our experiences elsewhere in the basin, we would expect there to be an orthogonal fault system offsetting the basement through the Permian part of the section and for that pattern to be reflected in the depositional patterns and fracture patterns of the overlying units. We are unable to demonstrate such a relationship based on the findings of this investigation.

With the notable exception of the basin margin thrust fault, we have found no relationship of faulting in the Fruitland Formation with structure at depth in the study area but the data we had to work with are somewhat limited and do not allow for unambiguous interpretations. Several critical structures , such as the problematic north-south oriented faulting, could be easily resolved with a tie line or two and a small 3-D survey in the area of interest would undoubtedly resolve a number of the questions. We do not have enough

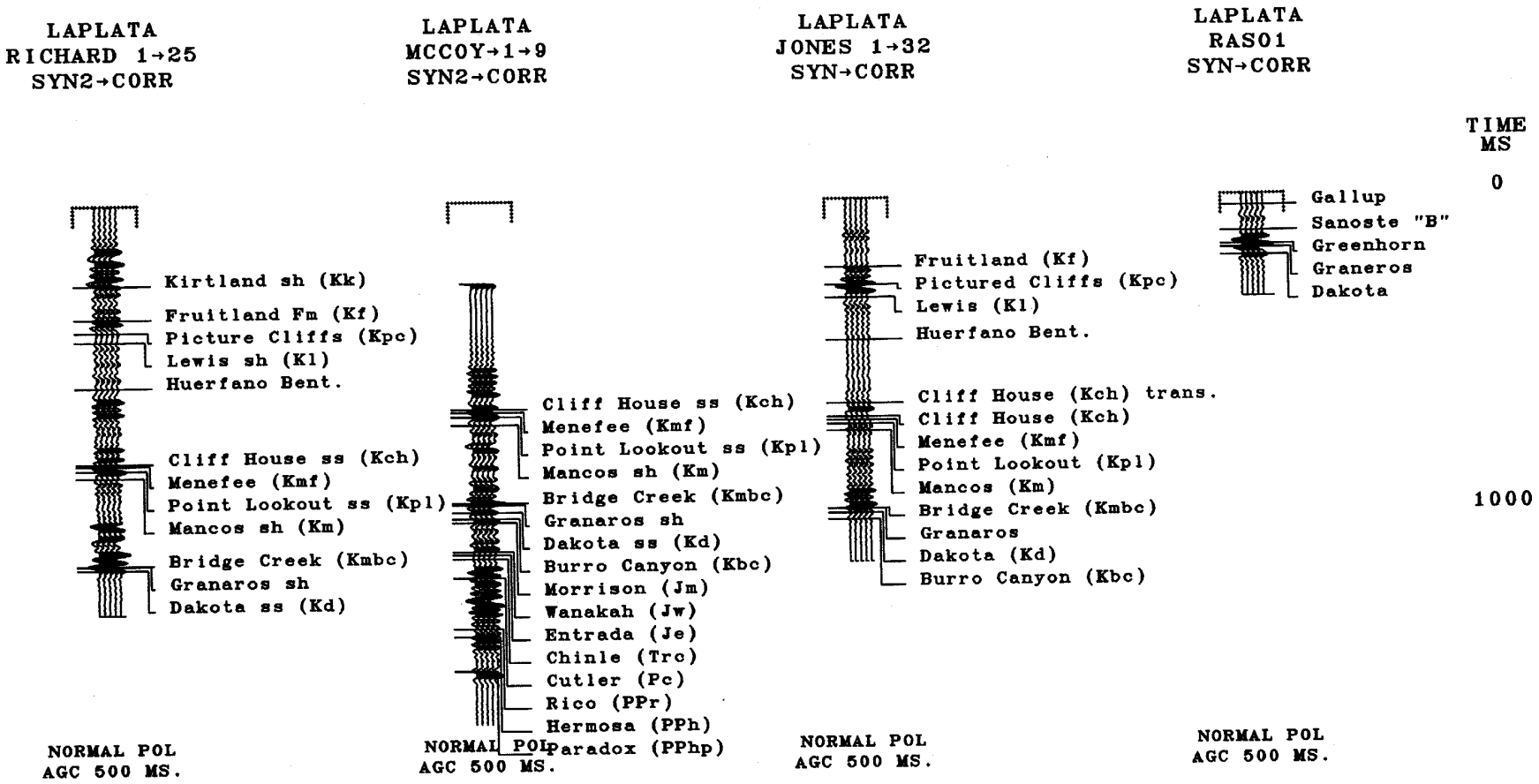

Figure 3-7. Display of the synthetic seismograms and the picked geologic horizons interpreted from the well information for each of the wells used in the study.

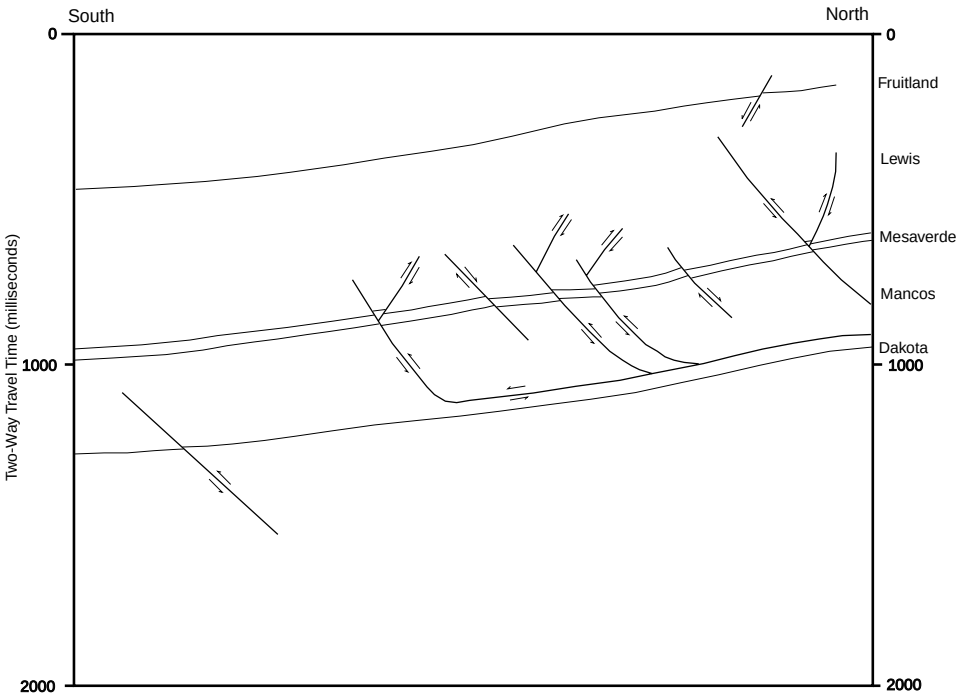

Figure 3-8. Line Drawing Interpretation of Amoco line HSX-1.

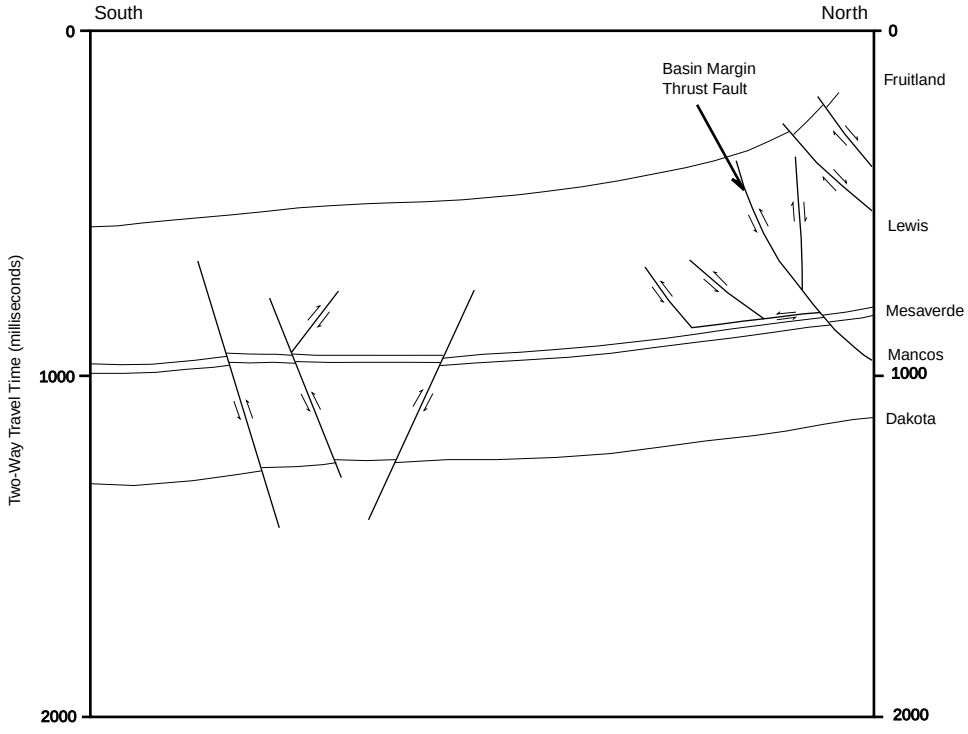

Figure 3-9. Line Drawing Interpretation of Amoco line HSX-2.

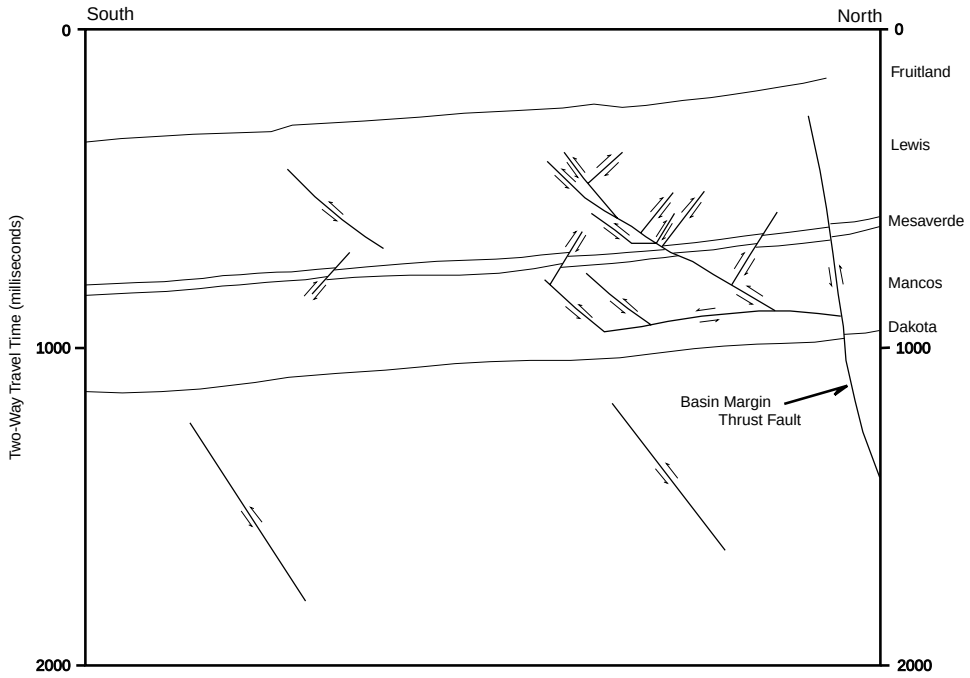

Figure 3-10. Line Drawing Interpretation of Amoco line HSX-3.

data in the right location to say there is or is not a pattern of faulting in the Fruitland that reflects the orthogonal basement pattern we have seen elsewhere in the basin.

The following is a summary of our principal conclusions:

1. The Dakota Sandstone is a strong continuous reflector with few offsets at a scale resolvable by the Amoco seismic data provided for this study.
2. The Fruitland Formation is a strong continuous reflector with few offsets at a scale resolvable by the Amoco seismic data.
3. In this area, the entire Cretaceous section, including the Fruitland, is offset by the basin margin thrust faults.
4. Much of the movement on the basin margin thrust is apparently taken up along a detachment surface in the lower Mancos and along related thrusts and back thrusts in the Mancos and Lewis Shales.
5. The Mesaverde is extensively broken and offset by the thrusts and back thrusts.
6. It is impossible to determine the pattern of faulting and its relationship to fracturing in the Cretaceous without more data, particularly some lines at right angles to the existing data.

ACKNOWLEDGMENTS

We are grateful to Amoco Production Company, Maxus Exploration Company, and K.N. Energy, Inc. for providing the data necessary for this study. We also benefited from discussions with a number of people, particularly Harry TerBest, Tom Ann Casey, and Curt Johnson, as well as from review comments by Chris Potter and John Miller. The interpretations and conclusions expressed, however, are ours alone.

REFERENCES CITED

Faust, L.Y., 1951, Seismic velocity as a function of depth and geologic time: Geophysics, v. 16, no. 2, p. 192-206.

Faust, L.Y., 1953, A velocity function including lithologic variation: Geophysics, v. 18, no. 2, p. 271-288.

Huffman, A.C., Jr., and Condon, S.M., 1993, Stratigraphy, structure, and paleogeography of Pennsylvanian and Permian rocks, San Juan Basin and adjacent areas, Arizona, Colorado, New Mexico, and Utah: U.S. Geological Survey Bulletin 1808-O, 44 p., 18 pl.

Huffman, A.C., Jr., and Taylor, D.J., 1989, San Juan Basin faulting—more than meets the eye

(abs): American Association of Petroleum Geologists Bulletin, v.73, no. 9, p. 1161.
Huffman, A.C., Jr., and Taylor, D.J., 1991, Basement fault control on the occurrence and development of San Juan Basin energy resources (abs): Geological Society of America Abstracts with Programs: v. 23, no. 4, p. 34.
Lindseth, R.O., 1979, Synthetic sonic logs—a process for stratigraphic interpretation: Geophysics, v. 44, no. 1, p. 1-26.
Taylor, D.J., and Huffman, A.C., Jr., 1988, Overthrusting in the northwestern San Juan Basin, New Mexico—A new interpretation of the Hogback Monocline, in Programs and Abstracts, 1988 McKelvey Forum: U.S. Geological Survey Circular 1025, p. 60-61.